Solid Earth Discuss., 4, 1545–1584, 2012
www.solid-earth-discuss.net/4/1545/2012/
doi:10.5194/sed-4-1545-2012

Solid Earth
Discussions

Effects of fire on ash thickness in a Lithuanian grassland and short-term spatio-temporal changes

P. Pereira[1], A. Cerdà[2], X. Úbeda[3], J. Mataix-Solera[4], D. Martin[5], A. Jordán[6], and M. Burguet[7]

[1]Department of Environmental Policy, Mykolas Romeris University, Ateities g. 20, 08303 Vilnius, Lithuania
[2]Departament de Geografia. Universitat de Valencia. Blasco Ibàñez, 28, 46010 Valencia, Spain
[3]GRAM (Mediterranean Environmental Research Group), Dept of Physical Geography and Regional Geographic Analysis, University of Barcelona, Montalegre, 6, 08001 Barcelona, Spain
[4]Environmental Soil Science Group. Department of Agrochemistry and Environment, Miguel Hernández University, Avda. de la Universidad s/n, Elche, Alicante, Spain
[5]USGS, 3215 Marine Street, Boulder, Colorado, USA
[6]MED_Soil Research Group, University of Sevilla, C/Profesor García González, s/n. 41012, Sevilla, Spain

[7]Institute for Sustainable Agriculture (IAS-CSIC), Department of Agronomy, University of Cordoba, Av. Menendez Pidal s/n Campus Alameda del Obispo, Apartado 4084, 14080, Córdoba, Spain

Received: 30 November 2012 – Accepted: 6 December 2012 – Published: 18 December 2012

Correspondence to: P. Pereira (pereiraub@gmail.com)

Published by Copernicus Publications on behalf of the European Geosciences Union.

Abstract

Ash thickness is a key variable in the protection of soil against erosion agents after planned and unplanned fires. Thicker ash provides better protection against raindrop impact and reduces the runoff response by retaining water and promoting water infiltration although little is known about the distribution and the evolution of the ash layer after the fires. Ash thickness measurements were conducted along two transects (flat and sloping areas) following a a grid experimental design. Both transects extended from the burned area into an adjacent unburned area. We analysed ash thickness evolution according to time and fire severity. In order to interpolate data with accuracy and identify the techniques with the least bias, several interpolation methods were tested in the grid plot. Overall, the fire had a low severity. The fire significantly reduced the ground cover, especially on sloping areas owing to the higher fire severity and/or less biomass previous to the fire. Ash thickness depends on fire severity and is thin where fire severity was higher and thicker in lower fire severity sites. The ash thickness decreased with time after the fire. Between 4 and 16 days after the fire, ash was transported by wind. The major reduction took place between 16 and 34 days after the fire as a result of rainfall, and was more efficient where fire severity was higher. Between 34 and 45 days after the fire no significant differences in ash thickness were identified among ash colours and only traces of the ash layer remained. The omni-directional experimental variograms shown that variable structure did not change importantly with the time, however, the most accurate interpolation methods were different highlighting the slight different patterns of ash thickness distribution with the time. The ash spatial variability increased with the time, particularly on the slope, as a result of water erosion.

1 Introduction

After fire, especially in severe crown fires and in grassland fires, the ash and the remaining vegetation cover on the soil surface are the main protection against erosion

agents. The amount of charred litter and ashes have been found to be a key factor in reducing post-fire soil erosion risk (Cerdà and Doerr, 2008; Zavala et al., 2009) during a range of time that can vary between some days and months (Cerdà, 1998; Marcos et al., 2000; De Luis et al., 2003). The period of time that ashes remain on the soil surface depends on the rainfall characteristics and the ash properties (Cerdà and Doerr, 2008). The characteristics of the ash depend upon the burned plant species, amount of biomass, fuel moisture content, temperature peaks and residence time (Ulery et al., 1993; Úbeda et al., 2009; Pereira et al., 2009). Also, it is widely recognized that ash is an important source of nutrients for post-fire ecosystem recuperation (Mataix-Solera et al., 2009). Ash is an important source of Ca, Mg and K, but also of some micronutrients that could act like contaminants such as Al, Mn, Fe and Zn (Pereira et al., 2010). Ash also plays an important role in post-fire runoff and erosion. Some studies have shown that ash can enhance runoff and erosion by sealing the soil surface (Gabet and Sternberg, 2008; Onda et al., 2009) and occluding soil pores (Lavee et al., 1998), or decrease runoff as result of water storage (Cerdà and Doerr, 2008; Woods and Balfour, 2008; Zavala et al., 2009), or both (Woods and Balfour, 2010). For example, Woods and Balfour (2010) observed that a <1 cm ash layer overlying a coarse soil led to clogging of the larger pores, enhancing the runoff response in relation to pre-fire conditions. On the other hand, the same ash overlying a fine textured soil did not have any effect on pore clogging. After a prescribed fire, Zavala et al. (2009) found that the thickness of the ash layer was positively correlated to time required for ponding and runoff initiation during rainfall simulations, as well as contributed to decreased runoff rate. Cerdà (1998) and Cerdà and Doerr (2008) found that the infiltration rates of recently fire-affected soils were high due to the protective cover of the ash. These authors observed that ash layer water storage increased with ash thickness and that this storage likely prevented or reduced runoff.

Fire induces mineralization of organically bound N, P and base cations which become available for plants or are leached through soil (DeBano et al., 1998). Little is known about the effects of ash thickness on the nutrients in runoff. However, Bodí et al. (2011a) did not find any differences between the nutrient flux in runoff from ash with ash depths of 5, 15 and 30 mm, suggesting that the concentration of cations in runoff from ash layers easily reaches saturation.

Soil protection by ash and vegetative residues is of major importance until vegetation recovers (Cerdà 1998a; Woods and Balfour, 2008). In addition ash is an important source of nutrients for vegetation recovery (Pereira et al., 2012a). The capacity of ash to protect soil depends upon the topography of the burned area, meteorological conditions during the post-fire and ash thickness. High fire severity can reduce the thickness of the litter layer cover (Cerdà and Doerr, 2008; Pereira et al., 2010). Several studies have been conducted on the effects of ash on soil properties in burned areas (Mallik et al., 1984; Leighton-Boyce et al., 2007; Cerdà and Doerr, 2008; Gabet and Sternberg, 2008; Onda et al., 2008; Woods and Balfour, 2008, 2010; Larsen et al., 2009; Zavala et al., 2009) and some of these studies considered ash thickness as a key to understand the post-fire ecosystem evolution due to the influence of ashes on soil fertility, and soil and water conservation. We consider that thickness of the ash layer is of major importance for soil protection from runoff and erosion because of the reasons mentioned above. Nevertheless, few studies have been conducted on the spatial and temporal evolution of ash thickness and the factors that control this evolution (Pereira et al., 2012b). This is probably due to the fact that ashes are ephemeral features of fire-affected landscapes. Larsen et al. (2009) reported that a 5-mm-thick ash was easily eroded by rainfall, and a thicker layer is unlikely to persist much longer due to wind and runoff after the first few storms (Cerdà and Doerr, 2008; Onda et al., 2008). This also explains that ash studies are not so developed and considered novel within the forest fire research topics. In addition, the mentioned studies did not make comparisons with control adjacent areas, that allow identify the impact of fire in soil protection. The study of ash thickness shows the degree of soil protection in the immediate period after the fire, and how it changes in space and time. This has implications on quickly changing soil nutrient status, due to ash removal, ash erosion, infiltration and type of ash. With ash, nutrients are also transported.

After a laboratory experiment, Liodakis et al. (2009) observed that the amount of most nutrients extracted in successive leachates from *Pinus halepensis* and *Quercus coccifera* ash samples during sequential extraction under the weak acidic conditions of rainwater (pH = 6) is progressively reduced. These results might have implications on the type and amount of elements leached in a certain place, which could be different according to ash composition. Thus ash mobility after fire has important implications on soil properties and a better understanding of ash movement in soil is important and necessary. The primary factors that control ash thickness are the spatial variability of fuels and fire severity. After fire, it has been observed that the ash layer is gradually reduced (Bodí et al., 2011b) and (re)distributed at different rates as a result of the effects of erosion by wind and water, topography of the burned area, dissolution, compaction, and incorporation into the soil profile. The heterogeneous ash thickness decrease and ash redistribution has important implications on ash spatial variability, thus on soil protection and impact on physical and chemical properties (Cerdà and Doerr, 2008; Pereira et al., 2010; Zavala et al., 2009).

Using interpolation methods to understand the spatial distribution of environmental variables and their pattern across the landscape can result in significant effort, budget and time saving. Mapping variables involves estimating values at not sampled areas by mean of interpolation methods. However, the effectiveness of mapping depends on the accuracy of the spatial interpolation as mentioned in several studies, which also discuss the most appropriate methods for the interpolation of variables (Schloeder et al., 2001; Erxleben et al., 2002; Robinson and Metternicht, 2006; Simbahan et al., 2006; Sun et al., 2009; Erdogan, 2009; Palmer et al., 2009; Xie et al., 2011). Independently of the scale of analysis, accurate spatial predictions are fundamental in the evaluation of the effects of fire on the landscape and strategies to mitigate its impacts. Some studies have been conducted on the spatial distribution of ash properties after fire and have shown that these can be highly variable, even at plot scale. The spatial variability of ash thickness may be affected by intrinsic factors such as soil properties and ash texture, which depend on fire temperature, fire severity, vegetation moisture content, amount and type of biomass and fuel distribution; and extrinsic factors such as wind, water erosion and rain splash (Pereira et al., 2010).

This study aims to quantify the spatial and temporal distribution of ash thickness in the immediate period following low severity grassland fire in boreal ecosystem of Lithuania and study the main controlling factors. Ash thickness was analysed in two areas with different topography (flat and slope), using different methodologies for data collection (transect and grid sampling). In transect-sampling areas, ash thickness was compared with the adjacent non-burned litter layer in order to quantify the impact of low severity fire in soil protection; in the grid-sampling area several interpolation methods were tested. In addition, fire severity was calculated according to ash colour, as used by several authors (Smith and Hudak, 2005; Goforth et al., 2005; Pereira et al., 2012).

2 Materials and methods

2.1 Study site and data collection

The study area is located near Vilnius (Lithuania), approximately in the coordinates 54.42° N/25.26° E, and 154 m a.s.l., in an urban/forest interface area. The fire started by 14 April 2010, after unknown causes and affected approximately 4 ha of a recently abandoned agricultural area. The soil is developed on glacio-fluvial sediments and is classified according to FAO as a *Cambic Arenosol* (Kadunas et al., 1999). Based on the analysis of 15 samples collected in the study area, soil texture is composed of 86 % sand, 6 % silt and 8 % clay. According to the Vilnius weather station (267 300-EYVI, data between 1955 and 2012), mean annual temperature is 6.3 °C, mean annual rainfall is 809.1 mm (rainfall and/or snow). Annual and spring prevailing winds are from the northwest (Bukantis, 1994). The vegetation is mainly composed of common dandelion (*Taraxacum officinale*) and buffalo grass (*Anthoxanthum odoratum).*

Prior to the ash thickness measurements, we established two transects that included part of the burned area and part of the control-unburned area: the first transect,

west-to-east oriented, in a flat area with a total length of 181 m (101 m in the burned area and 81 m in the control area); the second transect, in a south-facing slope with an inclination of 14 %, was 114 m long (62 m in the burned area and 53 m in the control area). Ash thickness measurements required several precautions. Previously to measurements of ash and litter thickness, routes were stablished in order to avoid errors in the determination of ash thickness due to stepping. For both transects we first selected a starting point and marked it carefully. Subsequently we measured the ash thickness every 100 cm using iron bars 50 cm long. Marks were placed every 200 cm in order to avoid errors in locating the measurement points. Ash thickness was measured only after careful verification of transect length and mark locations.

Additionally, north-south oriented $27 \times 9\,\text{m}^2$ grids were disposed on part of the burned area, and 40 samples were collected every 3 m (in this case control points were placed every 3 m). Coordinates of the sample points were determined using a GPS device. Ash thickness was determined as described above. More detailed information about ash thickness measurements is available in Cerdà and Doerr (2008), Pereira et al. (2010) and Woods and Balfour (2010). Fire severity was classified using ash colour, as proposed by Úbeda et al. (2009). Ash thickness determinations were carried out 4, 16, 34 and 45 days after fire, until vegetation covered most of the soil surface.

In order to determine the effects of precipitation on the dynamics of the thickness of the ash layer and vegetation recovery, daily rainfall data from the Vilnius weather station (Zirmunai, 54.41° N/25.17° E, 148 m a.s.l.), 1 km far from the study area were recorded and analyzed.

2.2 Statistical analysis

Prior to data analysis, normality of data and homogeneity of variances were checked with the Shapiro-Wilk (Shapiro and Wilk, 1965) and the Levene test, respectively. Normal distribution and homogeneity of variances were considered at a $p > 0.05$. Since most of the variables did not satisfy these assumptions (even after logarithmic and

Box-Cox transformations; Box and Cox, 1964), non-parametric Friedman ANOVA test was used. An analysis of the ash thickness differences within ash colour in each sampling period was carried out with the non-parametric test Kruskall-Wallis ANOVA test (K-W). When ANOVA null hypothesis was rejected ($p < 0.05$), pos-hoc pairwise comparisons were performed to investigate differences between means (Tukey HSD post-hoc test; Conover, 1980; Sokal and Rohlf, 1995). The comparison between transects was carried out with the non-parametric factorial ANOVA test on rank-transformed data because the normality and homogeneity of the variances were not achieved, even after the ln and Box-Cox transformations. A similar procedure was applied to compare ash thicknesses among sampling periods in the grid area. However, with the exception of ash thickness measured 16 days after fire, all data fitted the normal distribution. After logarithmic (natural logarithm) transformation all distributions fitted the Gaussian distribution. Thus, repeated ANOVA tests were applied. When significant differences were identified ($p < 0.05$), Tukey HSD test was applied. All graphics in the figures are presented with original data. All statistical analyses were performed with STATISTICA 6.0 (Statsoft Inc) and SPSS 18.0.

2.3 Spatial structure, interpolation methods and assessment criterion

Spatial patterns of ash thickness in the grid area were observed with variogram modelling for evaluating the spatial continuity of ash thickness among data points and identify the range of spatial dependence. In this study the modelled variograms are omni-directional (which considers that the variability is equal in all directions) because, according to Webster and Oliver (2007), at least 150 data points are needed to reliably identify the presence of anisotropy. When possible, variable dependence was calculated with the Nug/sill ratio. According to Chien et al. (1997), if the variable has strong, moderate or weak spatial dependence (ratios < 25 %, 25–75 % and > 75 %, respectively. Strong spatial dependence is commonly attributed to intrinsic factors and weak spatial dependence to extrinsic factors (Cambardella et al., 1994).

To characterize the spatial variation of ash thickness in the grid area, several well-known interpolation methods were tested in order to identify the most accurate one. This methodology has been applied previously to studies of ash (Pereira and Úbeda, 2010), soil properties (Robinson and Metternicht, 2006) and precipitation distribution (Diodato and Ceccarelli, 2005; Moral, 2010). The interpolation methods vary in their assumptions, from global to local perspectives, and whether processes are deterministic or stochastic in nature. For more detailed information interested readers can consult Isaaks and Srivastava (1989), Goovaerts (1999), Webster and Oliver (2007) or Smith et al. (2009). In this study we tested interpolation precision with nine interpolation methods: the deterministic methods Inverse Distance to a Power (IDP), with the power of 1, 2, 3, 4 and 5, Local Polynomial (LP) with the power of 1 and 2, Spline with Tension (SPT), Completely Regularized Spline (CRS), Multiquadratic (MTQ), Inverse Multiquadratic (IMQ) and Thin Plate Spline (TPS). Some geostatistical methods were also used: Ordinary Kriging (OK) and Simple Kriging (SK). For each interpolation method we considered a total of 15 neighbours and applied a smoothing factor (0.5). These interpolation methods we used are extensively described in the literature (Chaplot et al., 2006; Yilmaz, 2007; Smith et al., 2009; Pereira and Úbeda, 2010; Pereira et al., 2010; Xie et al., 2011). The interpolation methods assessment criterion was based on the errors produced by each method (Observed-Predicted) observed with the cross-validation method. With these data we calculate the mean error (ME) and root mean square error (RMSE).

The best interpolation method is the one that has the lowest RMSE. Further explanations of these indexes can be found in Mardikis et al. (2005), Pereira and Úbeda (2010), and Pereira et al. (2010). In addition we compared the observed and estimated distributions with a paired t-test ($p < 0.05$), and Pearson correlation coefficients ($p < 0.05$) were determined. Variograms were performed with Surfer 9.0 (Golden Software) and interpolation tests with ArcGis 9.3 (ESRI), for Windows.

3 Results

3.1 Rainfall post-fire

The first rainfall event (0.5 mm) occurred 8 days after fire. Between 4 and 16 days after the fire, cumulated rainfall was 9.5 mm. The major amount of rainfall was observed between 16 and 34 days after the fire (81 mm), mainly in the 25th day after the fire (31 mm in 24 h). Between 34 and 45 days after fire the amount of rainfall was 36 mm. Total rainfall during the study period was 121 mm (Fig. 1).

3.2 Flat area

In the flat area transect, ash colour was classified in three classes: black (51.96 %), dark grey (19.61 %) and light grey (28.43 %). The Friedman ANOVA results showed significant differences between litter or ash thickness data in time ($p < 0.001$; Table 1). Ash thickness decreased with time, more intensely between days 16 and 34 after fire. Nevertheless, this reduction was different according to fire severity (in terms of ash colour), as shown in Fig. 2, especially 4 (K-W = 62.23, $p < 0.001$) and 16 days after fire (K-W = 37.37, $p < 0.001$). Significant differences between ash colours were not observed between days 34 ($p > 0.05$) and 45 ($p > 0.05$) after fire. The evolution of ash thickness in time at the flat transect profile from the burned and control areas is shown in Fig. 3. The thickness of the ash layer increased between days 4 and 16 in some points. We did not identify any measured point without ash cover 4 and 16 days after fire. The bare soil surface was exposed only in some points by days 34 and 45 (17.50 % and 40 % respectively). The coefficient of variation (CV %) was 37.05 % in the control, 40.60 % (4 days after fire), 46.30 % (16 days), 86.97 % (34 days), and 113.48 % (45 days).

3.3 Slope area

In the slope transect ash was classified in four colour classes: black (40.94 %), dark grey (29.03 %), white (16.13 %) and light grey (12.90 %). The Friedman ANOVA results showed significant differences between litter and ash thickness ($p < 0.001$). As in the flat transect, the main differences in ash thickness were observed between days 16 and 34 after fire (Table 2). Differences among ash colours were registered in the first two ash thickness measurements, 4 (K-W = 51.27, $p < 0.001$) and 16 days after fire (K-W = 29.20, $p < 0.001$). Between 34 (K-W = 3.38, $p > 0.05$) and 45 days (K-W = 3.11, $p > 0.05$) no differences were identified (Fig. 4). Figure 5 shows the ash thickness profile for the sampling periods and in the control area. As in the flat area, the major reduction occurred 34 days after fire. As in the flat transect we identified some points where ash was thicker in the second measurement. On the slope transect all measured points were still covered by ash 4 days after fire. No ash layer was observed in 11.47 % of studied points 16 days after fire, and the bare surface increased to 52.45 % (34 days) and 67.21 % (45 days). The CV % was of 33.42 % in the control, 57.52 % 4 days, 69.73 % 16 days, 133.04 % 34 days, and 167.01 % 45 days after fire.

The comparison between sites showed significant differences between days (F = 246 699.20, $p < 0.001$), site (F = 13 272.23, $p < 0.001$) and the interaction between days and place (F = 12.94, $p < 0.001$). The thickness of the litter layer was higher in the flat area than in the sloped area and at 4 and 16 days after fire the ash layer was significantly thicker in the flat area. After this period no significant differences were observed in ash thickness in time and between the flat and slope transects (Fig. 6).

3.4 Grid area

Black (57.50 %) and dark grey (42.50 %) ash colour classes were identified in the grid area. The results of the ANOVA test showed significant differences in ash thickness for different ash colour classes (F = 5.80, $p < 0.05$), days (F = 328.80, $p < 0.001$) and ash colour and days (F = 6.31, $p < 0.05$). The greatest reduction of ash thickness was observed between days 16 and 34 after fire and no significant differences were observed between these (Fig. 7). As in the flat transect, all measured points 4 and 16 days after fire were covered by ash. Only 34 and 45 days after fire some points were bare (17.50 % and 40 % respectively). The CV % was of 34.39 % (4 days after fire), 37.19 % (16 days), 75.86 % (34 days), and 99.10 % (45 days). The temporal and spatial evolution of vegetation recover in the grid area is shown in Fig. 8. It is clear that the burned area recovered quickly, especially one month after fire (Fig. 8c). Forty-five days after fire, hardly any visual vestiges of fire impact remained.

The linear model is the best fit for the experimental variogram calculated for ash thickness measured 4 days after fire (Fig. 9a) and presents a nugget effect of 13.35 and a slope of 1.42 (Table 3). Sixteen and 45 days after fire, the linear model was also the one that fits better with the calculated experimental variograms (Fig. 9b and d) and shows a nugget effect of 7.31 and 0.80 and a slope of 0.60 and 0.49, respectively (Table 3). The spherical model fits perfectly with the experimental variogram calculated with the data collected 34 days after fire and shows a nugget effect of 0.80, a sill of 6.90 along a range of 7.22 m. The nug / sill ratio (0.11) showed that the variable has a strong spatial dependence.

Prior to the ash thickness modelling we tested the normality of data distribution. The next step was to test, using the normalized data, several interpolation methods and model their spatial distribution. The data of the ash measurements of 4, 34 and 45 days after fire had a Gaussian distribution. Sixteen days after fire data normality was only achieved after logarithmic transformation. Thus in this case we used ln transformed data for modelling.

The results of the tested interpolation methods for all measurement periods are shown in Table 4. Four days after fire, LP1 was the most accurate for interpolating the ash thickness (RMSE, 4.323) and the least precise was TPS (RMSE, 6.394) (Table 4a), 16 after fire, the most precise technique was SK (RMSE, 0.3464) and the least accurate was the LP2 (RMSE, 0.4700) (Table 4b), 34 days most accurate was IMTQ (RMSE, 1.802) and the least precise was IDW1 (RMSE, 2.144) (Table 4c) and 45 days

the most accurate method was CRS (RMSE, 0.6706) and the least precise was IDW1 (RMSE, 0.8686) (Table 4d). Method tests were considered unbiased, since ME is always very close to 0 (ranging between −0.06172 and 0.0469) and no differences were observed and predicted values (Table 4). Four days after fire, the correlation coefficient between observed and predicted values was only significant in LP1, meanwhile 16 days after fire significant correlations were observed between the two distributions in most methods (non significant correlations were observed in IDW1, IDW2, LP2 and TPS). Thirty four days after fire the correlations were significant in all techniques tested and 45 days, only IDW1 correlations between observed and predicted values were not significant (Table 4).

The spatial interpolation of ash thickness data was carried out with the most accurate method for each date, identified in the previous section. Results are shown in Fig. 10. Four days after fire, a decreasing trend in ash thickness from northeast to southwest of the plot was observed (Fig. 10a). Sixteen days after fire, the ash thickness persisted according to the previously identified trend in the north-eastern and central parts of the plot, while the thickness of the ash layer decreased in the eastern and south-eastern part of the plot. Thirty-four days after fire the ash distribution pattern changed substantially. The eastern part of the plot was thinner at some points when compared to the south-eastern, western and north-western parts of the plot. In the last ash thickness measurement date (45 days after fire) only trace amounts of ash remained and no ash cover was observed at a great number of points. Thicker ash deposits were identified in the eastern part of the plot and the areas without ash cover were in the north-eastern and south-western portions of the plot.

4 Discussion

Ash is a key variable for soil protection and landscape recuperation after fire. Some studies have reported ash thicknesses up to 70 mm in an oak forest burned by wildland fires (Ulery et al., 1993), 6 cm in a mixed pine forest (Goforth et al., 2005), and 17 mm in a mixed fir and larch forest (Woods and Balfour, 2008). Some authors have studied the relationship between ash cover and burn severity. Lewis et al. (2006), for example, concluded that more ash is present in moderate- and high-severity burns; but little information is available about fire severity effects on ash thickness and its temporal evolution (Pereira et al., 2012b), and no studies were done on this topic on boreal grassland ecosystems.

The studied area showed low severity burning, nevertheless, induced a significant reduction on ground cover. Ash colour is a key variable to understand fire severity (Smith and Hudak, 2005; Goforth et al., 2005; Úbeda et al., 2009). The intensity of combustion of organic matter ranges from scorching (producing black ash) to complete (producing white ash), depending on fire severity, moisture content and thickness of the organic layer (DeBano et al., 1998; Neary, 2004). Colour is a clear tracer of ash thickness as we observed here, in agreement previous research developed on Mediterranean-type ecosystems (Pereira et al., 2012b). In all studied plots, the black ash layer was thicker than the light grey or white ash layers because the lower degree of combustion leaves a greater amount of organic material remaining in the black ash layer. In both planned and unplanned burning, fire severity is very heterogeneous across the landscape and depends on the fuel type, structure, distribution, moisture, topography and meteorological conditions (Knapp and Keeley, 2006; Keeley, 2009). Fire severity was higher in the sloped area than in the flat areas, indicated by the presence of white ash. Fires tend to burn upslope and steeper slopes will burn with a higher intensity because the heat released during burning will pre-heat the fuel prior to combustion. In addition fire is very likely to be more severe on sloping areas, where the soil moisture content is smaller than in flat areas (Maingi and Henry, 2007). The slope where we measured ash thickness was south facing, thus more exposed to radiation. Also the original vegetation height and thickness of the litter layer were small in comparison with some parts in the flat burned area, based on measurements from the control area. It can be suggested that vulnerability to fire was high (Fig. 6).

Sixteen days after fire, a reduction of thickness of the ash layer was observed in all studied areas. In some points, ash cover decreased, and in other, the ash layer was thicker than in the previous determinations. The reduction of ash cover was observed especially where light grey and white ash were identified. Between 4 and 16 days after fire, no significant storms occurred. So, it is very likely that wind erosion induced the transport and redistribution of ash sediments through landscape and contributed to reduction of ash thickness (Fig. 1). Although wind has been reported as an important cause of ash redistribution (Notario del Pino et al., 2008; Whicker et al., 2006; Zavala et al., 2009; Pereira et al., 2012b), this question needs further detailed studies, since it was not possible collect wind data in the studied area. Due is probably another factor that contribute to the changes in the ash morphology and depth, but again no information is found on this topic in the scientific literature.

The major reduction in mean thickness of the ash layer, observed between days 16 and 34 after fire, was caused by erosion and compaction of the ash layer by rainfall. Other studies have already pointed out that rainfall plays an important role in controlling the decrease in ash thickness after fire (Cerdà, 1998a, b; Pereira et al., 2010a). It is very likely that rain splash contributed to compaction of the ash layer (Onda et al., 2008) and wind promoted transport, redistribution and incorporation into the soil profile (enhanced by the absence of trees that could intercept rain drops) that was particularly effective in locations where fire severity was higher. High severity fires reduce surface fuels to small particulates that are easy to transport and incorporate into the soil profile. Thus, it is very likely that ash produced at higher temperatures during burning induced the first effects on soil properties, since smaller particles are more easily incorporated into the underlying soil. Bioturbation may also contribute to reduction, redistribution and incorporation of ash into the soil profile. Soil invertebrates can survive after grassland fire, which rarely affect these populations (Neary et al., 1999). Wikars and Schimmel (2001) observed that fire impacts on invertebrates depend on the amount of organic matter consumed. Invertebrates living in deeper soil layers are less affected than those on the surface. The authors observed that after fire.

Rapid recolonization by some species of beetles (*Atomaria pulchra*, Cryptophagidae; or *Corticaria rubripes*, Lathridiidae) was observed by authors. After experimental burnings in Australian tropical savanna, Jerome and Andersen (2001) observed that beetle abundance was higher in burned plots than in the control. Ants also contribute to remove or cover ashes from the soil surface (Cerdà and Doerr, 2010). This is due the intense activity of ants after forest fires (Pereira et al., 2012b). The lack of ash at some sampling points after 34 days after fire may be also a result of these processes.

Ash incorporation into the soil profile also depends on soil properties, mainly texture (Woods and Balfour, 2010). It is expected that incorporation of ash into the underlying sandy soil in the study area probably happens readily. Between days 36 and 45 after fire, the reduction of ash thickness might be a result of ash compaction and soil infiltration, since vegetation recovery (probably a result of the timing of the fire during the growing season and to the incorporation of ash nutrients into the soil profile), reduced wind impact (Fig. 10c and d). Ash depletion happened quickly on the sloping area.

The omni-directional experimental variograms allow us to understand the spatial structure of ash thickness in the studied periods. For days 4, 16 and 45 after fire, a linear model showed the best fit, suggesting that the spatial variability of the variable increased with distance and the range of variance was not reached inside the studied area. This situation was not observed 34 days after fire, where the variogram showed a great spatial dependence (Table 6) which suggests that ash thickness was controlled by intrinsic factors (e.g., soil properties and ash texture), that enhanced ash infiltration. The vegetation recuperation in this period might reduce the impact of wind and rain on ash dynamics and favoured infiltration of fine ash particles into the soil porous media. The spatial structure of the ash thickness distribution in the grid area was very similar and changed little during the study because no significant water flow and transport occurred in the flat area, enhancing incorporation of ashes into the soil profile.

The test of the different interpolation methods allows us to have an accurate idea of the spatial distribution of ash thickness after fire. Four days after fire we observed that LP1 was the most precise method. LP methods are sensitive to neighbouring distance

and they are especially accurate when data vary in a short range (Smith et al., 2006). Consequently, if data do not have significant spatial variations, LP may be considered a good interpolator. LP interpolation gives us indirect evidence of the probable fire line progression from northeast to south-west and the attendant fire severity. Litter consumption is a tracer of fire severity and temperature as identified elsewhere (Úbeda et al., 2009). It is also widely recognized that fire temperature rises with the distance covered by the fire line (Marcelli et al., 2002; Gimeno-Garcia et al., 2004), especially if vegetation structure and composition are homogeneous, as observed in the control area.

For data collected 16 days after fire, the most accurate method was SK. Kriging and/or other geostatistical methods rely on the theory of regionalized variables which assumes that the variability of data is homogenous across the studied area (Webster and Oliver, 2007). Thus we observed that ash thickness follows a determined spatial pattern that was easily identified with SK. No major changes were identified in ash thickness between 4 and 16 days after fire. Since little rainfall occurred, it is very likely that the spatial distribution of the ash thickness was affected by wind transport and may have impact also in other areas outside the burned plot. However, the fire severity was low in this grassland fire, and wind transport of relatively large ash particles is expected to be less effective than wind erosion of finer particles produced during high severity wildland fires (Pereira et al., 2012b). Thirty four and 45 days after fire, the most accurate interpolation methods were IMTQ and CRS, and the integrated group of Radial Basis Functions that are deterministic interpolators (not based on regional patterns). Some local patterns are distinguished that are very likely to be induced by different rates of ash incorporation into the soil profile at the different measured points.

Soil protection is more variable in the burned area than in control. Fire creates a highly variable pattern of ash distribution, due the different conditions of combustion. As expected, this variability increases with time especially in the sloping area where runoff flow and wind erosion are more efficient. Reduced thickness of the ash layer and the increase of spatial variability will induce a heterogeneous soil protection pattern over time, varying as a result of ash compaction and redistribution. This means that soil is differentially exposed to erosion agents, showing high small-scale variability with implications for the spatial pattern of the post-fire hydrological response. In our experiment, erosion was not a major problem, because of the rapid vegetation regrowth. Also, runoff patterns can be substantially changed as a result of ash thickness variability. For example, runoff decreased in areas where the ash layer was thicker, as observed by Cerdà and Doerr (2008) and Woods and Balfour (2010). The increase of ash spatial variability with time will have also important implications on the type and amount of nutrients availability for plant growth (Pereira et al., 2012a).

5 Conclusions

The study of the spatio-temporal evolution of ash thickness is relevant in order to assess the degree of soil protection after fire and the major factors affecting this evolution. The studied fire was of low severity, yet it produced a significant reduction in vegetation cover, especially in the sloping area, owing to lower fuel amounts previous to the fire and/or higher fire severity such as the ash colour shown.

Ash was reallocated by wind after during the first two weeks after fire and later the rainfall and the subsequent surface wash compacted the ash. After 34 days, ash dissolution and infiltration and the burrowing by fauna was probably the main disturbance of the ash layer. Vegetation recovered very fast and soil was rapidly protected from erosion, even after the ash thickness decreased. The interpolation methods carried out allow us to estimate indirectly the probable fire line evolution, which was from north-east to south-west and attendant fire severity during the first post-fire measurements. Ash spatial variability increased over time, especially in the sloping area as a result of water erosion.

Acknowledgements. The authors acknowledge the Spanish Ministry of Science and Innovation for funding projects CGL2007-28764-E/BTE CGL2008-01632-E/BTE and CGL2009-06861-E/BTE, and supporting the Spanish Network on the Effects of Wildfires on Soils (FUEGORED); the Lithuanian Research Council for financing the project Fire effects on Lithuanian soils and ecosystems (LITFIRE, MIP-48/2011); the Spanish Ministry of Economy and Competitiveness for funding the HYDFIRE project (CGL2010-21670-C02-01); the Comissionat per a Universitats i Recerca del DIUE de la Generalitat de Catalunya; the Lithuanian Hydrometereological Service for providing climate data; and the Cerdocarpa Team for the important suggestions to this manuscript.

References

Bodí, M., Leon Miranda, F. J., Cerdà, A., Balfour, V., Mataix-Solera, J., and Doerr, S.: Runoff rates, water erosion and water quality from a soil covered with different types of ash, in: Fire effects on soil properties, edited by: Bento Gonçalves, A. and Vieira, A., Proceedings of the 3rd International meeting of fire effects on soil properties, Guimaraes, Portugal, 64–67, 2011a.

Bodí, M., Mataix-Solera, J., Doerr, S., and Cerdà, A.: The wettability of ash from burned vegetation and its relationship to Mediterranean plant species type, burn severity and total organic carbon content, Geoderma, 160, 599–607, 2011b.

Box, G. E. P. and Cox, D. R.: An analysis of transformations, J. Roy. Stat. Soc. B, 26, 211–252, 1964.

Bukantis, A.: Lietuvos klimatas, Vilniaus Universitetas, leidykla, Vilniaus, 1994.

Cambardella, C. A., Moorman, T. B., Novak, J. M., Parkin, T. B., Turco, R. F., and Konopka, A. E.: Field scale variability of soil properties in central Iowa soils, Soil Sci. Soc. Am. J., 58, 1501–1511, 1994.

Cerdà, A.: Postfire dynamics of erosional processes under mediterranean climatic conditions, Z. Geomorphol., 42, 373–398. 1998a.

Cerdà, A.: Changes in overland flow and infiltration after a rangeland fire in a Mediterranean scrubland, Hydrol. Process., 12, 1031–1042, 1998b.

Cerdà, A. and Doerr, S. H.: The effect of ash and needle cover on surface runoff and erosion in the immediate post-fire period, Catena, 74, 256–263, 2008.

Cerdà, A. and Doerr, S. H.: The effect of ant mounds on overland flow and soil erodibility following a wildfire in eastern Spain, Ecohydrology, 3, 392–401, 2010.

Chaplot, V., Darboux, F., Bourennane, H., Leguédois, S., Silvera, N., and Phachomphon, K.: Accurancy of interpolation techniques for derivation of digital elevation models in relation to landform types and data density, Geomorphology, 77, 126–476, 2006.

Chien, Y. L., Lee, D. Y., Guo, H. Y., and Houng, K. H.: Geostatistical analysis of soil properties of mid-west Taiwan soils, Soil Sci., 162, 291–298, 1997.

Conover, W. J.: Practical nonparametric statistics, Wiley, New York, 1980.

DeBano, L. F., Neary, D. G., and Ffolliott, P. F.: Fire's Effects on Ecosystems, Wiley, 1998.

Diodato, N. and Ceccarelli, M.: Interpolation processes using multivariate geostatistics for mapping of climatological precipitation mean in the Sannio mountains (Southern Italy), Earth Surf. Proc. Land., 30, 259–268, 2005.

Erdogan, S.: A comparison of interpolation methods producing digital elevation models at field scale, Earth Surf. Proc. Land., 34, 366–376, 2009.

Erxleben, J., Elder, K., and Davies, R.: Comparison of spatial interpolation methods for estimating snow distribution in the Colorado Rocky Mountains, Hydrol. Process., 16, 3627–3649, 2002.

Gabet, E. J. and Sternberg, P.: The effects of vegetative ash on infiltration capacity sediment transport and generation of progressively bulked debris flows, Geomorphology, 101, 666–673, 2008.

Gimeno-Garcia, E., Andreu, V., and Rubio, J. L.: Spatial patterns of soil temperatures during experimental fires, Geoderma, 118, 17–38 2004.

Goforth, B. R., Graham, R. C., Hubbert, K. R., Zanner, C. W., and Minnich, R. A.: Spatial distribution and properties of ash and thermally altered soil properties after high-severity forest fire, Int. J. Wildland Fire, 14, 343–354, 2005.

Goovaerts, P.: Geostatistics in soil science: state of art and perspectives, Geoderma, 89, 1–45, 1999.

Isaaks, E. H. and Srivastava, R. M.: An Introduction to Applied Geostatistics, Oxford University Press, 1989.

Kadunas, V., Budavicius, R., Gregorauskiene, V., Katinas, V., Kliaugiene, E., Radzevicius, A., and Taraskevicius, R.: Geochemical Atlas of Lithuania, Lithuanian Geological Survey, 1999.

Keeley, J. E.: Fire intensity, fire severity and burn severity: a brief review and suggested usage, Int. J. Wildland Fire, 18, 116–126, 2009.

Knapp, E. E. and Keeley, J. E.: Heterogeneity in fire severity within early season and late season prescribed burns in a mixed-conifer forest, Int. J. Wildland Fire, 15, 37–45, 2006.

Larsen, I., MacDonald, L. H., Brown, E., Rough, D., Welsh, M. J., Pietraszek, J. H., Libohava, Z., Benavides-Solorio, J. D., and Schaffrath, K.: Causes of post-fire runoff and erosion: water repellency, cover, or soil sealing?, Soil Sci. Soc. Am. J., 73, 1393–1407, 2009.

Lavee, H., Kutiel, P., Segev, M., and Benyamini, Y.: Effect of surface roughness on runoff and erosion in a Mediterranean ecosystem: the role of fire, Geomorphology, 11, 227–234, 1998.

Leighton-Boyce, G., Doerr, S. H., Shakesby, R. A., and Walsh, R. P. D.: Quantifying the impact of soil water repellency on overland flow generation and erosion: a new approach using rainfall simulation and wetting agent on in situ soil, Hydrol. Process., 21, 2337–2435, 2007.

Lewis, S. A., Wu, J. Q., and Robichaud, P. R.: Assessing burn severity and comparing soil water repellency, Hayman Fire, Colorado, Hydrol. Process., 20, 1–16, 2006.

Liodakis, S., Tsoukala, M., and Katsigiannis, G.: Laboratory study of leaching properties of Mediterranean forest species, Water Air Soil Poll., 203, 99–107, 2009.

Maingi, J. K. and Henry, M. C.: Factors influencing wildfire occurrence and distribution in eastern Kentucky, USA, Int. J. Wildland Fire, 16, 23–33, 2007.

Mallik, A. U., Gimingham, C. H., and Rahman, A. A.: Ecological effects of heather burning. I. Water infiltration, moisture retention and porosity surface soil, J. Ecol. 72, 787–776, 1984.

Marcelli, T., Santoni, P. A., Simeoni, A., Leoni, E., and Porterie, B.: Fire spread across pine needle fuel beds: characterization of temperature and velocity distributions within the fire plume, Int. J. Wildland Fire, 13, 37–48, 2002.

Marcos, E., Tarrega, R., and Luis-Calabuig, E.: Comparative analysis of runoff and sediment yield with rainfall simulator after experimental fire, Arid Soil Res. Rehab., 14, 293–307, 2000.

Mardikis, M. G., Kalivas, D. P., and Kollias, V. J.: Comparison of interpolation methods for the prediction of reference evapotranspiration – An application in Greece, Int. Ser. Prog. Wat. Res., 19, 251–278, 2005.

Mataix-Solera, J., Guerrero, C., Arcenegui, V., Bárcenas, G., Zornoza, R., Perez-Bejarano, A., Bodí, M. B., Mataix-Beneyto, J., Gómez, I., Garcia-Orenes, F., Navarro-Pedreño, J., Jordán, M. M., Cerdà, A., Doerr, S. H., Úbeda, X., Outeiro, L., Pereira, P., Jordán, A., and Zavala, L. M.: Los incendios forestales y el suelo: un resumen de la investigación realizada por el Grupo de Edafología Ambiental de la UMH en colaboración con otros grupos, in: Efectos de los incendios forestales sobre los suelos en España, El estado de la cuestión visto por los científicos españoles, edited by: Cerdà, A. and Mataix-Solera, J., Càtedra de Divulgació de la Ciència, Universitat de Valencia, 185–217, 2009.

Moral, F. J.: Comparison of different geostatistical approaches to map climate variables: application to precipitation, Int. J. Climatol., 30, 620–631, 2010.

Neary, D. G.: An overview of fire effects on soils, Southwest Hydrology, September/October, 18–19, 2004.

Neary, D. G., Klopatek, C. C., DeBano, L., and Ffolliott, P. F.: Fire effects on bellow ground sustainability: a review and synthesis, Forest Ecol. Manag., 122, 51–71, 1999.

Notario del Pino, J., Dorta Almenar, I., Rodríguez Rodríguez, A., Arbelo Rodríguez, C., Navarro Rivero, F. J., Mora Hernández, J. L., Armas Herrera, C .M., and Guerra García, J. A.: Analysis of the 1:5 soil: water extract in burnt soils to evaluate fire severity, Catena, 74, 246–255, 2008.

Onda, Y., Dietrich W. E., and Booker, F.: Evolution of overland flow after severe forest fire, Point Reyes, California, Catena, 72, 13–20, 2008.

Jerome, O. and Andersen, A. N.: Fire and biodiversity: responses of grass-layer beetles to experimental fire regimes in an Australian tropical savana, J. Appl. Ecol., 38, 49–62, 2001.

Palmer, D. J., Höck, B. K., Kimberley, M. O., Watt, M. S., Lowe, D. J., and Payn, T. W.: Comparison of spatial prediction for developing *Pinus radiata* productivity surfaces across New Zealand, Forest Ecol. Manag., 258, 2046–2055, 2009.

Pereira, P. and Úbeda, X.: Spatial distribution of heavy metals released from ashes after a wildfire, J. Environ. Eng. Land. Manag., 18, 13–22, 2010.

Pereira, P., Bodí, M., Úbeda, X., Cerdà, A., Mataix-Solera, J., Balfour, V., and Woods, S.: Las cenizas y el ecosistema suelo, in: Actualización en métodos y técnicas de estudio de los suelos afectados por incendios forestales, edited by: Cerdà, A. and Jordan, A., Càtedra de Divulgació de la Ciència, 345–398, 2010.

Pereira, P., Úbeda, X., Outeiro, L., and Martin, D.: Factor analysis applied to fire temperature effects on water quality, in: Forest Fires: Detection, Suppression and Prevention, Series Natural Disaster Research, Prediction and Mitigation, edited by: Gomez, E. and Alvarez, K., Nova Science Publishers, New York, 273–285, 2009.

Pereira, P., Ubeda, X., and Martin, D. A.: Fire severity effects on ash chemical composition and extractable elements, Geoderma, 191, 105–114, 2012a.

Pereira, P., Cerdà, A., Úbeda, X., Mataix-Solera, J., Arcenegui, V., Zavala, L.: Modelling the impacts of wildfire on ash thickness in a short-term period, Land Degrad. Dev., accepted, doi:10.1002/ldr.2195, 2012b.

Robinson, T. P. and Metternicht, G.: Testing the performance of spatial interpolation techniques for mapping soil properties, Comp. Electron. Agr., 50, 97–108, 2006.

Schloeder, C. A., Zimmerman, N. E., and Jacobs, M. J.: Comparison of methods for interpolating soil properties using limited data, Soil Sci. Soc. Am. J., 65, 470–479, 2001.

Shapiro, S. and Wilk, M.: An analysis of variance test for normality, Biometrika, 52, 591–611, 2001, 1965.

Simbahan, G. C., Dobermann, A., Goovaerts, P., Ping, J., and Haddix, M. L.: Fine-resolution mapping of soil organic carbon based on multivariate secondary data, Geoderma, 132, 471–489, 2006.

Smith, A. M. S. and Hudak, A. T.: Estimating combustion of large downed woody debris from residual white ash, Int. J. Wildland Fire, 14, 245–248, 2005.

Smith, M. P., Zhu, A. X., Burt, J. E., and Stiles, C.: The effects of DEM resolution and neighborhood size on soil digital survey, Geoderma, 137, 58–69, 2006.

Smith, M. J., Goodchild, M. F., and Longley, P. A.: Geospatial Analysis. A comprehensive guide to principles techniques and software tools, Troubador Publishing, Leicister, 2009.

Sokal, R. R. and Rohlf, F. J.: Biometry: the principles and practice of statistics in biological research, 3rd Edn., Freeman, San Francisco, 1995.

Sun, Y., Kang, S., Li, F., and Zhang, L.: Comparison of interpolation methods for depth to groundwater and its temporal and spatial variations in the Minqin oasis of Northwest of China, Environ. Modell. Softw., 24, 1163–1170, 2009.

Úbeda, X., Pereira, P., Outeiro, L., and Martin, D.: Effects of fire temperature on the physical and chemical characteristics of the ash from two plots of cork oak (*Quercus suber*), Land Degrad. Dev., 20, 589–609, 2009.

Ulery, A., Graham, R. C., and Amrhein, C.: Wood ash composition and soil pH following intense burning, Soil Sci., 156, 358–364, 1993.

Webster, R. and Oliver, M. A.: Geostatistics for environmen-tal scientists, Wiley Interscience, 2nd Edn., London, 2007.

Whicker, J. J., Pinder III, J. E., and Breshears, D. D.: Increased wind erosion from forest wildfire: Implications for contaminant-related risks, J. Environ. Qual., 35, 468–478, 2006

Wikars, L. O. and Schimmel, J.: Immediate effects of fire-severityon soil invertebrates in cut and uncut pine forests, Forest Ecol. Manag., 141, 189–200, 2001.

Woods, S. W. and Balfour, V. N.: The effect of ash on runoff and erosion after a severe forest wildfire, Int. J. Wildland Fire, 17, 535–548, 2008.

Woods, S. W. and Balfour, V. N.: The effects of soil texture and ash thickness on the post-fire hydrological response from ash-covered soils, J. Hydrol., 393, 274–286, 2010.

Xie, Y., Chen, T.-B., Lei, M., Yang, J., Guo, Q.-J., Song, Bo., and Zhou, X.-Y.: Spatial distribution of soil heavy metal estimated by different interpolation methods; Accurancy and uncertainty analysis, Chemosphere, 82, 468–476, 2011.

Yilmaz, H. M.: The effect of interpolation methods in surface definition: an experimental study, Earth Surf. Proc. Land., 32, 1346–1361, 2007.

Zavala, L. M., Jordán, A., Gil, J., Bellinfante, N., and Pain, C.: Intact ash and charred litter reduces susceptibility to rain splash erosion post-fire, Earth Surf. Proc. Land., 34, 1522–1532, 2009.

Table 1. Summary of Friedman ANOVA and Tukey HSD test, for ash thickness in a flat area in all measurement periods. Different letters mean significant differences at a $p < 0.05$. Data in mm.

	mean	SE	min	max	Friedman ANOVA
Control	119.5^a	5	45	210	Chi Sqr. = 308.04, $p < 0.001$
4 days	30.9^b	1.2	10	72	
16 days	22.2^c	1.0	2	49	
34 days	2.6^d	0.2	0	10	
45 days	1.1^d	0.1	0	5	

Table 2. Summary of Friedman ANOVA and Tukey HSD test, for ash thickness in slope area in all measurement periods. Different letters mean significant differences at a $p < 0.05$. Data in mm.

	Mean	SE	Min	max	Friedman ANOVA
Control	92.1^a	4.2	29	176	Chi Sqr. = 154.61, $p < 0.001$
4 days	23.1^b	1.7	3	53	
16 days	16.2^b	1.4	0	39	
34 days	2.2^c	0.4	0	8	
45 days	0.8^c	0.2	0	4	

Table 3. Best-fitted omnidirectional variogram models of ash thickness and corresponding parameters.

Time	Model	Nugget effect	Slope/ Sill	Range (m)	Nug/sill ratio
4 days	Linear	13.35	1.42	10	–
16 days	Linear	7.31	0.60	10	–
34 days	Spherical	0.80	6.90	7.22	0.11
45 days	Linear	0.30	0.49	10	–

Table 4. Summary statistics of the accuracy of interpolation methods. Numbers in bold indicate the least biased method. (A) 4 days after the fire, (B) 16 days after the fire, (C) 34 days after the fire and (D) 45 days after the fire. Correlations between observed and estimated values significant at * $p < 0.05$, ** $p < 0.01$, *** $p < 0.001$ and $^{\text{n.s}}$ not significant at a $p < 0.05$.

	Method	Min	Max	ME	RMSE	Obs vs. Est	r
(A)	IDW 1	−10.609	7.566	0.0195	4.572	0.9788	0.10 $^{\text{n.s}}$
	IDW 2	−10.961	7.246	−0.04	4.573	0.9567	0.16$^{\text{n.s}}$
	IDW 3	−11.223	7.019	−0.05922	4.662	0.9371	0.17$^{\text{n.s}}$
	IDW 4	−11.389	7.096	−0.06172	4.775	0.9360	0.16$^{\text{n.s}}$
	IDW 5	−11.490	7.424	−0.0602	4.867	0.9388	0.16$^{\text{n.s}}$
	LP 1	**−10.235**	**6.696**	**−0.03826**	**4.323**	**0.9562**	**0.35***
	LP 2	−12.131	8.971	0.03093	5.512	0.9722	0.03$^{\text{n.s}}$
	SPT	−10.911	6.912	−0.01973	4.661	0.9790	0.19$^{\text{n.s}}$
	CRS	−11.068	7.526	−0.02713	4.804	0.9720	0.17$^{\text{n.s}}$
	MTQ	−11.873	9.073	−0.05668	5.267	0.9467	0.12$^{\text{n.s}}$
	IMTQ	−10.542	7.362	0.0469	4.530	0.9847	0.17$^{\text{n.s}}$
	TPS	−12.466	11.040	−0.05317	6.394	0.9588	0.008$^{\text{n.s}}$
	OK	−10.791	6.946	0.01863	4.539	0.9796	0.22$^{\text{n.s}}$
	SK	−10.701	6.688	−0.03476	4.475	0.9615	0.25$^{\text{n.s}}$
(B)	IDW 1	−0.7715	0.7126	−0.003097	0.3609	0.9575	0.16$^{\text{n.s}}$
	IDW 2	−0.7754	0.7046	−0.007328	0.3514	0.8970	0.27$^{\text{n.s}}$
	IDW 3	−0.7750	0.7075	−0.007567	0.3480	0.8926	0.32*
	IDW 4	−0.7730	0.7134	−0.006422	0.3484	0.9089	0.33*
	IDW 5	−0.7711	0.7185	−0.005271	0.3497	0.9254	0.34*
	LP 1	−0.6446	0.7533	0.0386	0.3591	0.5036	0.33*
	LP 2	−0.8045	1.6942	0.008538	0.4700	0.9102	0.10$^{\text{n.s}}$
	SPT	−0.7200	0.7121	−0.001585	0.3475	0.9774	0.33*
	CRS	−0.7128	0.7121	−0.00147	0.3498	0.9791	0.34*
	MTQ	−0.7246	0.7008	0.0007356	0.3655	0.9900	0.32*
	IMTQ	−0.7283	0.7173	−0.0007262	0.3467	0.9896	0.33*
	TPS	−0.8182	0.8249	0.009062	0.3969	0.8873	0.30$^{\text{n.s}}$
	OK	−0.7411	0.7086	−0.007969	0.3488	0.8872	0.32*
	SK	**−0.7299**	**0.7068**	**−0.004116**	**0.3464**	**0.9412**	**0.34***

Table 4. Continued.

	Method	Min	Max	ME	RMSE	Obs vs. Est	r
(C)	IDW 1	−4.819	3.242	0.03467	2.144	0.9200	0.37*
	IDW 2	−4.323	3.104	−0.07788	1.944	0.8035	0.50***
	IDW 3	−4.301	3.114	−0.0571	1.916	0.8533	0.53***
	IDW 4	−4.156	3.086	−0.0641	1.879	0.8323	0.55***
	IDW 5	−4.077	3.066	−0.06249	1.863	0.8350	0.56***
	LP 1	−4.038	3.415	0.1101	1.856	0.7125	0.57***
	LP 2	−4.038	3.546	0.1242	1.897	0.6864	0.55***
	SPT	−3.679	3.005	−0.01504	1.811	0.9589	0.60***
	CRS	−3.721	3.016	−0.01452	1.809	0.9602	0.60***
	MTQ	−3.593	3.008	−0.015	1.832	0.9594	0.59***
	IMTQ	**−3.797**	**3.028**	**−0.009278**	**1.802**	**0.9745**	**0.60*****
	TPS	−3.853	3.460	0.02984	1.912	0.9228	0.59***
	OK	−3.641	3.105	−0.001916	1.813	0.9947	0.59***
	SK	−3.723	3.092	−0.04579	1.825	0.8762	0.58***
(D)	IDW 1	−1.960	1.086	0.04005	0.8689	0.774	0.31$^{\text{n.s}}$
	IDW 2	−1.826	1.103	0.006488	0.8141	0.960	0.45**
	IDW 3	−1.796	1.107	−0.01071	0.7907	0.933	0.48**
	IDW 4	−1.906	1.088	−0.01735	0.7827	0.890	0.50***
	IDW 5	−1.958	1.064	−0.01948	0.7793	0.876	0.51***
	LP 1	−1,852	1.393	−0.05376	0.8264	0.686	0.41**
	LP 2	−2.266	1.299	−0.01511	0.871	0.914	0.39*
	SPT	−1.903	1.162	−0.009115	0.7729	0.941	0.54***
	CRS	**−1.728**	**1.360**	**0.0007761**	**0.6706**	**0.994**	**0.72*****
	MTQ	−1.774	1.676	0.01107	0.7504	0.929	0.67***
	IMTQ	−1.898	1.174	−0.008938	0.7516	0.931	0.58***
	TPS	−2.482	1.462	−0.02202	0.8297	0.869	0.51**
	OK	−1.674	1.268	0.006854	0.7877	0.956	0.49**
	SK	−1.778	1.264	−0.004127	0.7846	0.973	0.50**

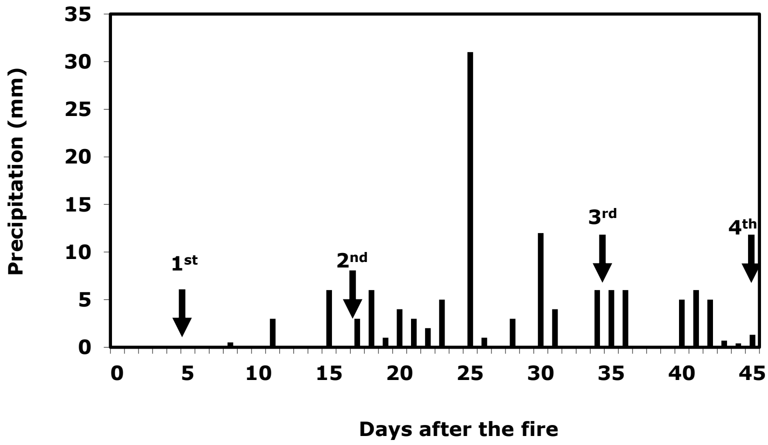

Fig. 1. Daily precipitation throughout the study period. Arrows point to days when measurements were collected and the numbers above the arrows indicate the measurement period.

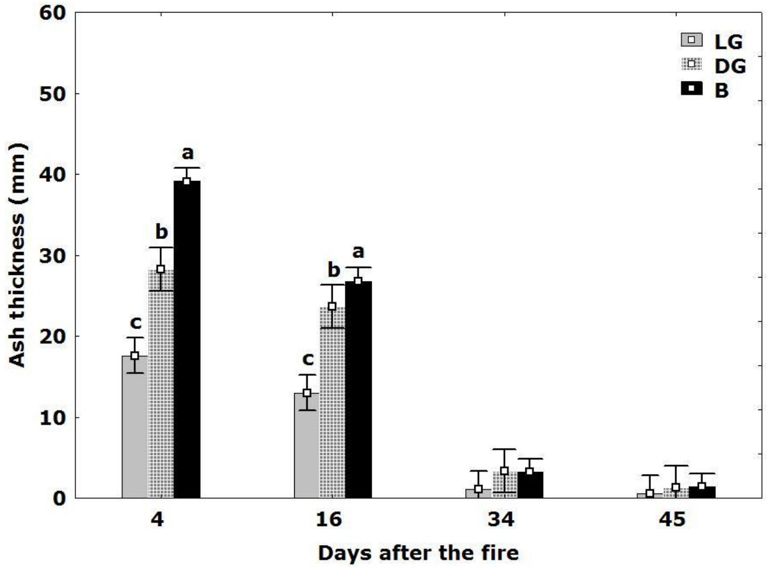

Fig. 2. Mean ash thickness in the flat area 4, 16, 34 and 45 days after the fire. Error bars indicate 95 % confidence interval. Different letters indicate significant differences ($p < 0.05$) between ash colors on each date (small letters).

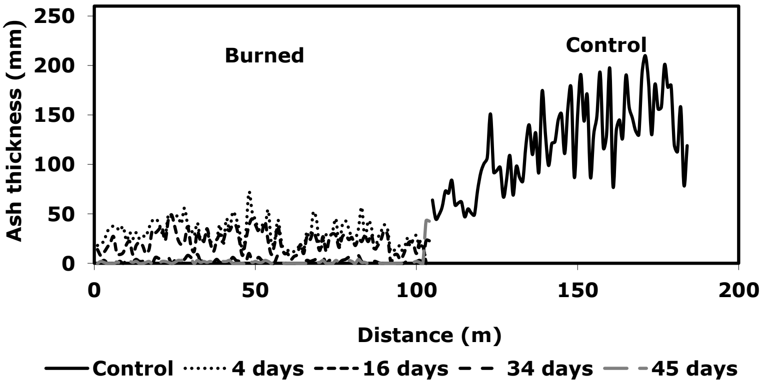

Fig. 3. Litter and ash thickness across all flat area transects in the different measurement periods (burned) and control area. The correlations only consider burned area. (Control $n = 80$, Burned plot $n = 101$)

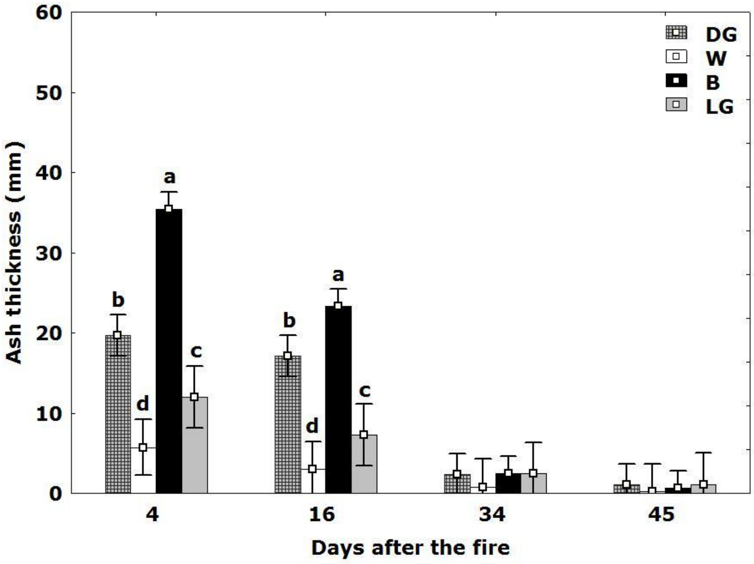

Fig. 4. Mean ash thickness in the slope 4, 16, 34 and 45 days after the fire. Error bars indicate 95 % confidence interval. Different letters indicate significant differences ($p < 0.05$) between ash colors on each date (small letters).

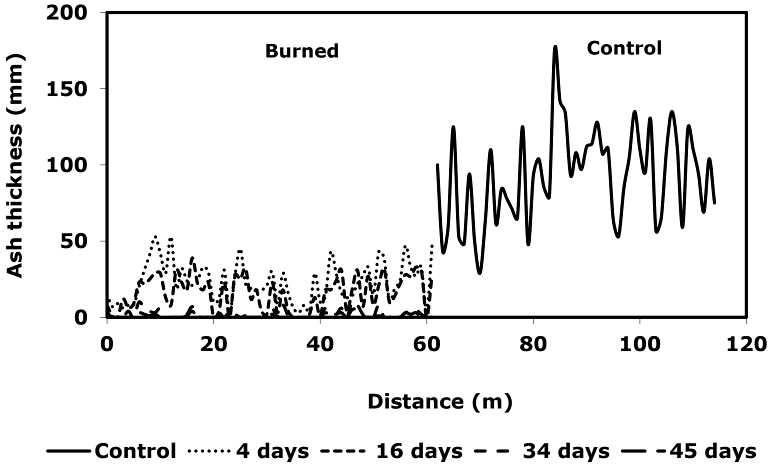

Fig. 5. Litter and ash thickness across the slope transects in the different measurement periods (burned) and control area. The correlations only consider burned area. (Control $n = 53$, Burned plot $n = 60$)

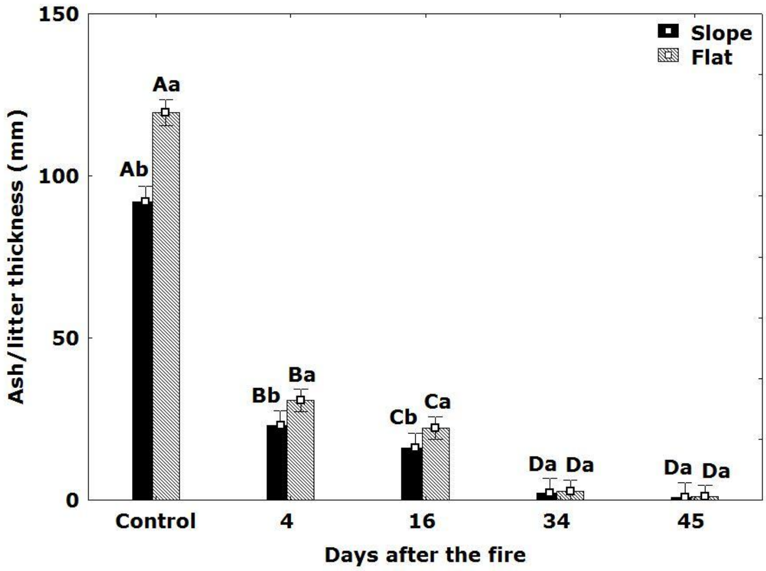

Fig. 6. Mean litter and ash thickness between flat and slope area 4, 16, 34 and 45 days after the fire. Error bars indicate 95 % confidence interval. Different letters indicate significant differences ($p < 0.05$) between measurement periods (capital letters) and between ash colors on each date (small letters). (a = higher mean, b = lower mean)

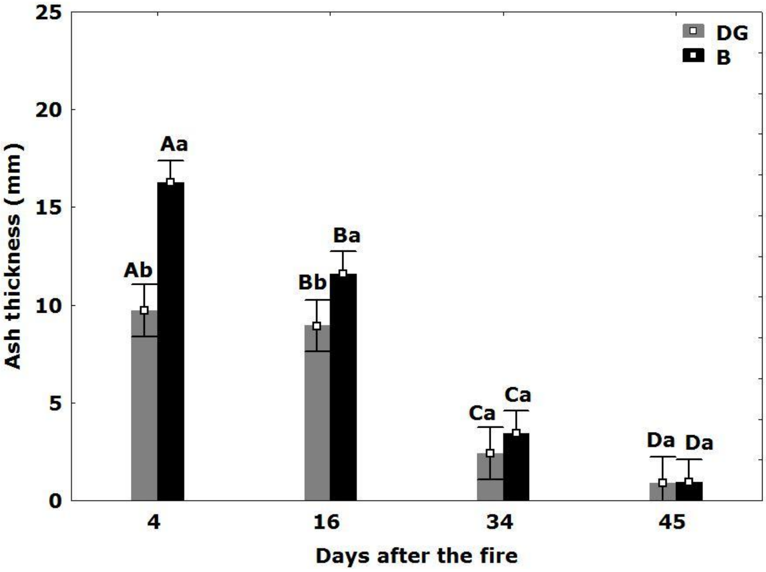

Fig. 7. Mean ash thickness in grid plot 4, 16, 34 and 45 days after the fire. Error bars indicate 95 % periods (capital letters) and between ash colors on each date (small letters). (a = higher mean, b = lower mean)

Fig. 8. From left to right and up down. View of the study site 4, 16, 34 and 45 days after the fire.

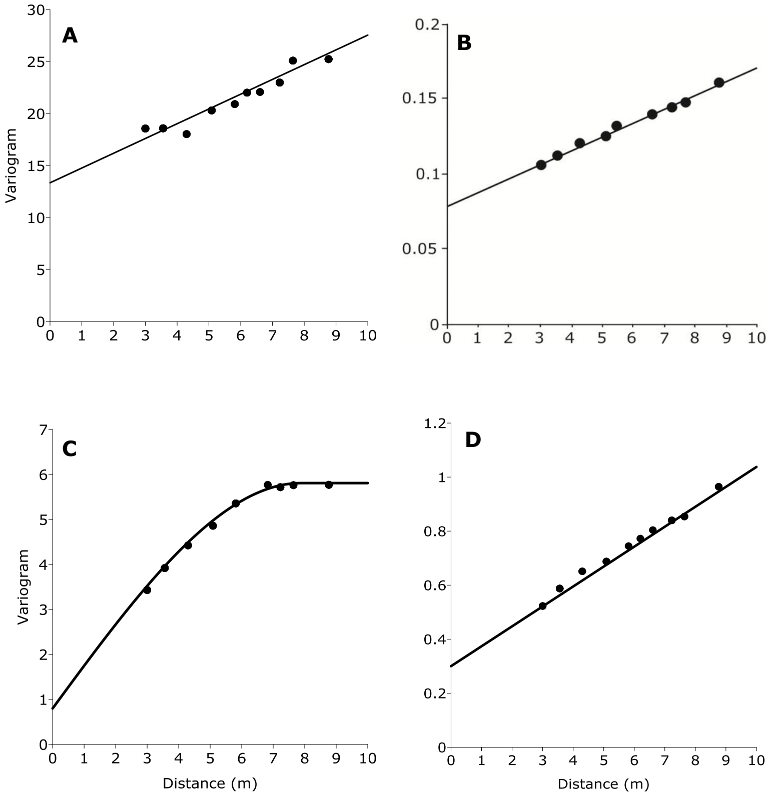

Fig. 9. Omni-directional variograms calculated for ash thickness distributions at **(A)** 4; **(B)** 16; with Ln data, **(C)** 34; and **(D)** 45 days after the fire.

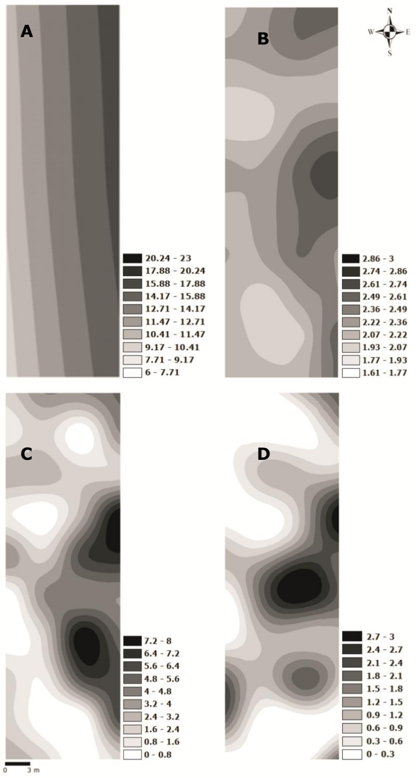

Fig. 10. Ash thickness interpolations according to the most accurate technique. From left to right. **(A)** 4 (LP1), **(B)** 16 (SK) with Ln data, **(C)** 34 (IMTQ) and **(D)** 45 days after the fire (CRS), data in mm, ln data for 16 day after the fire.